# EXPERIMENT ON INDUCED ACTIVITIES AND DECAY-HEAT IN SIMULATED D-T NEUTRON FIELDS: JAERI/USDOE COLLABORATIVE PROGRAM ON FUSION NEUTRONICS

Y. Ikeda, C. Konno and T. Nakamura
Department of Reactor Engineering,
Japan Atomic Energy Research Institute
Tokai-mura, Ibaraki-ken 319-11 Japan
0292-82-6016

A. Kumar and M. A. Abdou
University of California, Los Angeles
Los Angeles, CA 90024
U.S.A.
213-825-8266

## ABSTRACT

An experiment of Induced radioactivity and decayheat has been conducted in the framework of JAERI/USDOE collaborative program on the fusion blanket neutronics. Sixteen different materials have been irradiated in two typical DT neutron fields simulating spectra at the first wall and blanket regions of a fusion reactor. Induced radioactivity production profiles for both short and long irradiation times were analyzed by detecting associated γ-ray energy spectra. Energy release rate in material was characterized on the basis of the γ-ray emission data measured as well as β-ray contribution estimated. In this experimental study, focuses were placed not only on providing benchmark data for verification of the calculation code and nuclear data, but also on a comparative study for providing a guide line for the material selection concerning the dose rate as well as the decayheat after shutdown in the near term DT fusion devices.

## INTRODUCTION

Accurate estimation of radioactivity induced by DT neutron reactions is of importance because of its impact on nuclear design of DT burning fusion devices, e. g., ITER and FER. To meet the data requirement from the reactor design, an integral experiment has an important role to examine uncertainties in the calculation code and associated activation data. Benchmark experiments have been reported previously on the induced activities for SS-316 and concrete components [1-4] verifying the THIDA code system.[5]

Up to now, there have been much progress in the design and broad choice of the materials in the next generation fusion testing devices have been proposed. Thus, it is urgent requirement to establish more systematic data base pertinent to the induced radioactivity and decayheat assessment.

An integral experiment was conducted at the FNS facility[6] in the framework of JAERI/USDOE collaborative program on fusion neutronics during Phase-IIC[7]: the system for the coolant channel effect consisted of $Li_2O$ breeder blanket with a first wall enclosed by $Li_2CO_3$ with Polyethylene layer. The objectives of the experiment are to provide data for verifying radioactivity calculation codes, and to investigating the suitability of different materials in meeting the selection criteria based on low activation and decayheat considerations. The major independent variables considered in this study are materials, neutron spectrum, the operation time and the time after shutdown. Using experimental data, comparative investigation as material wise are performed in terms of γ-ray emission rate and total energy release rate as a function of neutron spectrum and irradiation and cooling time. The accompany paper[8] is treating successive experimental analysis using codes of THIDA2[9], REAC2[10] and DKRICF.[11]

## EXPERIMENTS

### Materials

Materials considered in the present study includes not only substantial structural materials of Iron, Nickel, Chromium, but the other potential materials of Aluminum, Silicon, Titanium, Molybdenum, etc.. Aiming at making a systematic experimental data base, sixteen different materials were chosen. In Table 1, they are shown together with their densities. To simplify the successive analysis, materials were to be single element rather than alloy. Only SS-316 and MnCu alloy(Mn 80%, Cu 20%) were selected because that SS-316 is one of most promising structural materials and Mn can not stand by itself as a metallic foil. The size of the sample was 5 mm in dia. by 1 mm in thickness except for Cr, Al, Si and W, which have dimensions of 12.7 mm in dia. by 0.1 mm in thickness for Al and W, and 10 $mm^2$ by 1 mm in thickness for Cr and Si.

Table 1. Materials tested and their densities

| Material name | Density($g/cm^3$) |
|---|---|
| Fe | 7.86 |
| W | 19.35 |
| Mo | 10.2 |
| V | 5.87 |
| SS-316 | 7.82 |
| Ni | 8.80 |
| MnCu | 8.60 |
| Co | 8.71 |
| Zr | 6.49 |
| Ti | 4.50 |
| Si | 2.42 |
| Al | 2.70 |
| Nb | 8.57 |
| Ta | 16.6 |
| Mg | 1.74 |
| Cr | 7.14 |

## Neutron Fields

Since neutron spectrum dependence on the radioactivity production is the fundamental parameter for the present investigation, the spectrum at the irradiation position is needed to be close to the realistic fusion neutron environment. The configuration of the Phase-IIC experimental assembly was chosen for this experiment. The system consisted of $Li_2O$ breeder blanket with a first wall enclosed by 200 mm $Li_2CO_3$ with 50 mm polyethylene. The DT neutron source was located in the cavity of the enclosure, at 780 mm distance from the first wall of the $Li_2O$ region. The cross sectional view of the system is shown in Fig. 1 along with two irradiation positions. The first sample location was set at 100 mm distance from the neutron source at 30° with respect to the incident $d^+$ beam direction. The other one was located at 50 mm depth in the $Li_2O$ region. As the first position(**A**) was close to the DT neutron source, it is expected that the neutron spectrum simulates a typical one at first wall region. The second position(**B**) provided simulation of typical spectrum inside tritium breeder blanket,$Li_2O$. Figure 2 illustrates neutron spectra calculated by DOT3.5 with GICX40 nuclear library,[12] which are to be used in the successive experimental analysis.[8] The spectrum inside the cavity includes neutron components reflected by the surrounding materials so that the field is expected reasonably to simulate the fusion radiation environment.

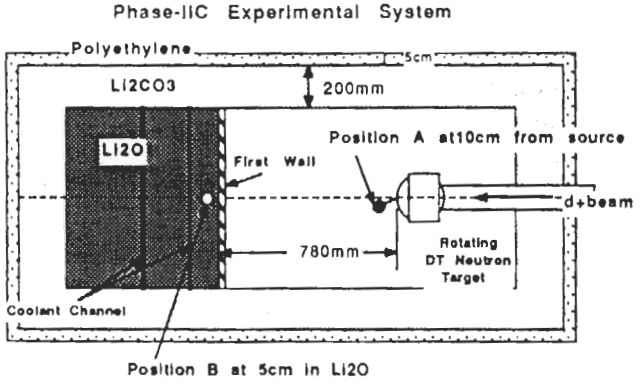


Fig. 1 The cross sectional view of Phase-IIC experimental system configuration and irradiation sample positions.

## Irradiations

One of parameters to be investigated here is a dependence of radioactivity on the time(the operation and cooling after shutdown). It is of importance because of inherent time dependent nature of the radioactivity. The variation in the plasma burning time and timing for the access after shutdown are very crucial to setup the experimental scenario for the testing of the devices.

Two irradiation times for 30 m and about 10 h were taken to respectively emphasize shorter and longer half-live products. The irradiation times for each irradiation runs are shown in Table 2 together with neutron source strengths. It is reasonably accepted to assume that the irradiation length for 30 min to 10 hours corresponds to the operation duration expected in the first stage of the testing devices.

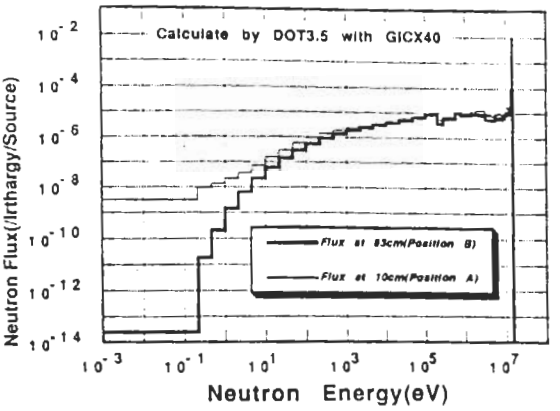


Fig. 2 Neutron energy spectra at the positions **A** and **B** calculated by DOT3.5 with GICX40 library.

Table 2. Irradiation times and neutron source strengths

| Run No. | Position | Irradiation Time | Source Strength |
|---|---|---|---|
| 1 | **A** | 30 m | $1.740 \times 10^{12}$/sec |
| 2 | **A** | 10 h | $9.046 \times 10^{11}$/sec |
| 3 | **B** | 30 m | $1.298 \times 10^{12}$/sec |
| 4 | **B** | 11 h | $1.022 \times 10^{12}$/sec |

## γ-ray spectrum measurements

After irradiation, samples were extracted from the system and γ-ray spectra were measured with four Ge detectors at cooling times ranging from10 m to 5 h for the short irradiation and 1 h to 7 days for the long irradiation. The data of cooling time and counting time for each run are described in detail in the accompany paper.[8] The γ-ray spectrum of Tungsten for the long irradiation at position **A** is shown in Fig. 3 as an example of the spectrum. The spectra measured were analyzed by a code BOB[13] to obtain γ-ray counts. Corrections for sum-peak, γ-ray self- absorption in the samples, material density, detector efficiency and neutron flux fluctuation were applied to obtain γ-ray spectra per unit volume. When the irradiation time is longer than the half-lives of the activities induced, correction for the neutron flux fluctuation during irradiation can not be negligible to keep assumption for the uniform strength irradiations.

Experimental errors estimated in the data processing are summarized in Table 3.

Table 3. Experimental error

| Error sources | Estimated value |
|---|---|
| Counting statistics | 0.1 to 50 % for single γ-ray<br>0.1 to 3 % for integrated |
| Detector efficiency | 2.5% for standard detector<br>3 - 4 % for relative detector |
| Self-absorption | 1 - 2 % |
| Neutron flux fluctuation | 0.5 - 2 % |
| Sum peak corrections | 1 - 2 % |

## RESULTS

### Materials Wise Observation

Identification of the decaying nuclide was performed using the decay γ-ray energy and relationship of their branching ratio.[14] In this section, the main contribution of activities for all spectra are described for each material.

**Fe:** For spectra at a cooling time less than 10 h by both short and long irradiations, $^{56}$Mn(T1/2=2.579h), the product by the reaction of $^{56}$Fe(n,p), has the largest contribution to the total γ-ray emission. The fraction of $^{54}$Mn(T1/2=312d), the product of $^{54}$Fe(n,p), increases as the cooling time increases longer than 1 day. No other activity was observed in this measurement. There was no significant spectrum dependence in those activity production rate except in the difference in the neutron flux level with respect to the distance to the source. This was due to that both production reactions are threshold type so that only the high energy neutron component contributed to the activity production.

**Ni:** Main contribution comes from $^{57}$Ni(T1/2=36h), the product of $^{58}$Ni(n,2n), in all spectra. In spectra for the short irradiation runs, $^{62m}$Co(T1/2=13.9m), the product of $^{62}$Ni(n,p), gave several % fraction to the total. For the long irradiation runs, $^{60}$Co(T1/2=5.271y), product of $^{60}$Ni(n,p), was observed though its contribution was small less than 1 %. The other nuclides observed were $^{57}$Co(T1/2=271d) and $^{58}$Co(T1/2=70.8d), the products from the decay of $^{57}$Ni + $^{58}$Ni(n,np), and $^{58}$Ni(n,p), respectively.

**Cr:** Spectra were measured only for the long irradiations. The 320 keV γ-line from $^{51}$Cr (T1/2=27.7d), the product of $^{50}$Cr(n,γ) and $^{52}$Cr(n,2n), was observed in both spectra. However, there was high intensity γ-line due to $^{34m}$Cl(T1/2=32m), which was produced by $^{35}$Cl(n,2n). This fact indicated that there was a certain amount of Cl as an unexpected impurity, which might be used as a coating material for Cr foil.

**Co:** The $^{56}$Mn, the products of $^{59}$Co(n,α), contributed 95 to 100 % and 10 to 80 % in spectra for the short and long irradiations, respectively. Contribution rate varied with the cooling time. The other nuclide observed were $^{59}$Fe(T1/2=44.6d) and $^{58}$Co, products of $^{59}$Co(n,p) and $^{59}$Co(n,2n), respectively. The $^{60}$Co of $^{59}$Co(n,γ) was observed in the spectrum for the long irradiation at the position **B**.

**Ti:** In the spectrum for the short irradiation at position **A**, annihilation 511 keV g-ray associated with $\beta^+$ decay of $^{45}$Ti(T1/2=3.1h), products of $^{46}$Ti(n,2n), occupied 40 % contribution to the total. The contribution of 511 kev γ-ray decreased to 6 % in the spectrum at position **B**. This is due to the fact that the direct 14 MeV neutron flux at position **B** is lower by two orders than that at position **A**. The $^{48}$Sc(T1/2=43.7h), the product of $^{48}$Ti(n,p) and $^{49}$Ti(n,np) gave the largest contribution through all measurements. The other nuclide observed in the spectra for the long irradiation were $^{47}$Sc (T1/2=3.42d) and $^{46}$Sc(T1/2=83.8d), products of $^{47}$Ti(n,p)+$^{48}$Ti(n,np) and $^{46}$Ti(n,p)+$^{47}$Ti(n,np), respectively.

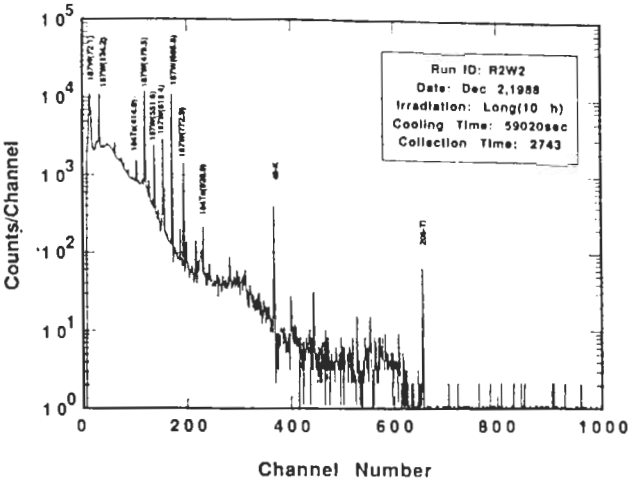


Fig. 3 Measured γ-ray spectrum of W sample for the long irradiation at position **A**.

**V:** In spectra for the short irradiations at both positions, $^{51}$Ti(T1/2=5.76m) gave the largest contribution of 60 to 80 % to the total and the next one was $^{48}$Sc, the product of $^{51}$V(n,α), showing about 20 % contributions. In the spectrum for the short irradiation at position **B**, $^{52}$V, the product of $^{51}$V(n,γ) was observed, the contribution of which was 18%, while only 1% in the spectrum at position **A**. This fact indicated the softness of the neutron spectrum at position **B**. In the spectra for the long irradiations, only $^{48}$Sc was observed.

**Mg:** Only spectra for the long irradiation runs were measured. Almost all contribution arose by $^{24}$Na (T1/2=15.02h), the products of $^{24}$Mg(n,p)+$^{25}$Mg (n,np).

**Al:** As the same situation as in the Mg, $^{24}$Na, the product of $^{27}$Al(n,α) dominated all spectra.

**Si:** Silicon is known as the low activation material because the reaction cross sections for the 14 MeV neutron are rather small and only short lived activities are produced. In this study, we could measure the spectrum only for the short irradiation at position **A**. Major activities were $^{27}$Mg(T1/2=9.46m) and $^{29}$Al(T1/2=6.6m), products of $^{30}$Si(n,α) and $^{29}$Si(n,p)+$^{30}$Si(n,np), respectively. They had contributions of 25 and 20 % to the total, respectively. However, as observed in the spectra for Cr, there were intense γ-lines from $^{34m}$Cl which contributed 55 % of the total.

**MnCu:** The spectrum for the short irradiation at position **A** gave strong annihilation γ-ray with 90 % contribution of the total γ-ray intensity. This was due to $^{62}$Cu(T1/2=9.73m), the product of $^{63}$Cu(n,2n). In the spectra at long cooling time, $^{64}$Cu(T1/2=12.7h), the product of $^{65}$Cu(n,2n) + $^{63}$Cu(n,γ), became the main source for the aniihillation γ-ray. At position **B**, $^{56}$Mn, the product of $^{55}$Mn(n,γ) had a contribution of 85 % for the short irradiation. For the long irradiation and long cooling time, $^{54}$Mn, the product of $^{55}$Mn(n,2n), dominated the spectrum with 70 % contribution.

**Zr:** Through all spectra, γ-ray from $^{89}$Zr(T1/2=78.4h), the product of $^{90}$Zr(n,2n), showed large

contributions of about 70 % to the total intensity. For the short irradiation, about 20 % contribution by $^{90m}$Y(T1/2=3.19h), the product of $^{90}$Zr(n,p) was observed. As the other activities, $^{87}$Sr(T1/2=2.8h), $^{91}$Sr(T1/2=9.5h), $^{91m}$Y(T1/2=49.7m) and $^{92}$Y(T1/2=3.54h) were identified. At position **B** for the long irradiation, a contribution of 9 % by $^{97}$Zr(T1/2=1.6h), the production of $^{96}$Zr(n,γ), was observed.

**Nb:** Gamma-lines from $^{92m}$Nb(T1/2=10.5d), the product of $^{93}$Nb(n,2n) dominated the spectrum in all cases. The other activity of $^{90m}$Y(T1/2=3.19h), the product of $^{93}$Nb(n,α), gave contributions of 1 to 15 %.

**Mo:** The main activity was $^{99}$Mo(T1/2=66.02h), the product of $^{98}$Mo(n,γ)+$^{100}$Mo(n,2n) and $^{99m}$Tc (T1/2=6.02h), the product of associated decay of $^{99}$Mo. THe same type of decay chain occurred in $^{101}$Mo(T1/2=14.6m),the product of $^{100}$Mo(n,γ), and $^{101m}$Tc(T1/2=14.2m), which were observed in the spectrum for the short irradiation at position **B**. In the spectrum for the short irradiation at position **A**, annihilation γ-ray occupied 50 % of the total intensity. The source of the annihilation was estimated to be mainly $^{91m}$Mo(T1/2=15.5m), the product of $^{92}$Mo(n,2n). The contribution decreased to be 17 % in the spectrum at position **B**. Other activities observed were $^{98m}$Nb(T1/2=51m), $^{97}$Nb(T1/2=72m), $^{96}$Nb(T1/2=23.4h), $^{93m}$Mo(T1/2=6.9h) and $^{92m}$Nb, the products of $^{98}$Mo(n,p), $^{97}$Mo(n,p), $^{96}$Mo(n,p), $^{92}$Mo(n,γ)+$^{94}$Mo(n,2n) and $^{92}$Mo(n,p),respectively.

**Ta:** Only spectrum for the long irradiation at position **B** was measured. Dominant activities were $^{182}$Ta (T1/2=115d), the product of $^{181}$Ta(n,γ), and $^{180m}$Ta(T1/2=8.1h), the product of $^{181}$Ta(n,2n), which gave contribution of 74 and 26 %. respectively.

**W:** Through all spectra, $^{187}$W(T1/2=23.9h), the product of $^{186}$W(n,γ), gave the largest contribution of more than 70 % to the total γ-ray intensities. Especially, it had more than 90 % contribution in the spectrum at position **B**. The other γ-lines were due to $^{184}$Ta (T1/2=8.7h), the product of $^{184}$W(n,p), $^{186}$Ta(T1/2=10.5m), the product of $^{186}$W(n,p), and $^{183}$Ta (T1/2=5.1d), the product of $^{183}$W(n,p).

**SS-316:** This is an alloy of Fe, Ni, Cr, Mn and Mo. The major activity was $^{56}$Mn; the product of $^{56}$Fe(n,p), showing contribution more than 90 % in the spectra at cooling time less than 1 day. For the short irradiation, $^{49}$Cr(T1/2=42.1m) was observed. Though the Mo constituent in SS-316 is small less than 3 %, γ-lines from $^{99}$Mo and $^{99\mu}$Tc were clearly detected. Other γ-lines from $^{57}$Ni, $^{58}$Co, $^{57}$Co were observed.

## DISCUSSION

It is primarily of importance to select materials which reduce the dose rate and decayheat after shutdown to the tolerable levels to meet the criteria from the safety point of view. In this study, an attempt was made to extract a guide line from the experiment for that purpose. In order to make a direct comparative study, the γ-ray emission rates at various cooling times were modified by using half-lives to be those at certain cooling times (at 1800 sec and 54000 sec for the short and long irradiations, respectively). These data were analyzed from view points of difference in neutron spectra at the irradiation positions and difference in irradiation time (short and long). Figure 4 shows ratios of γ-ray emission rate materials at position **B** to those at position **A**. In addition, the total energy release rate data are obtained directly from γ-ray emission rate data and indirectly from the β-ray branching ratio data taken from the Table of Isotopes.[13] The ratios Both γ-ray emission rates and energy release corresponding to respective irradiation runs are given in Figs. 5.1 to 5.4.

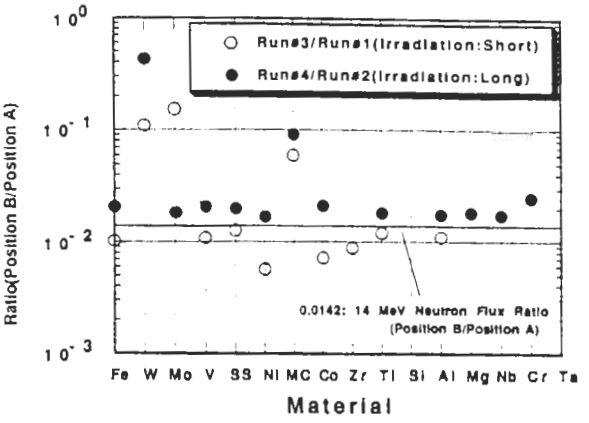


Fig. 4 Ratios of γ-ray emission rate materials at position **B** to those at position **A**.

### Neutron spectrum dependence

The ratios shown in Fig. 4 indicates the dependence of the γ-ray emission rates on the spectrum change for the materials. The ratios for almost all materials except W, Mo and MnCu in the both irradiations fall in the range from 0.008 to 0.02. Although the ratios at position **B** give slightly higher value systematically than those at position **A**, they are very close to the ratio of 0.014 for the neutron fluxes above 10 MeV at position **A** and **B**. This fact suggested that the radioactivity productions are governed by the reactions with primary DT neutrons in many materials.

As noted in the section for γ-ray spectrum observation, the presence of (n,γ) reaction obviously becomes dominant for several materials at position **B** where the 14 MeV neutron fraction is less than 10 % of the total and flux below 1 MeV occupy more than 50 %. It is significant for the materials of W, Mo and MnCu, the γ-ray spectrum of which are governed by $^{187}$W, $^{99}$Mo and $^{56}$Mn, the products of (n,γ) reaction, respectively.

As a result, it is concluded that not only 14 MeV neutrons, but also neutron reflected by the materials are highly important in the radioactivity assessment.

### Time dependence on the γ-ray emission rate

Comparisons of Fig 5.1 with 5.2 and Fig. 5.3 with 5.4, give the irradiation and cooling time dependencies on the γ-ray emission rate as a function of material. For the short irradiation at position **A**, Fe gives the highest γ-ray emission rate. MnCu, SS-316, Al and Co follow the Fe. On the other hand, for the long irradiation, Al and Mg show the largest value and Fe, SS-316 and MnCu give quite low value. This trend is reasonably accepted by considering the half-lives of the dominant activities and production cross

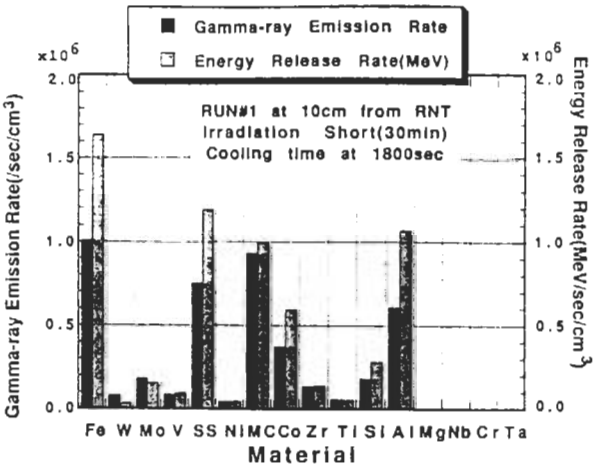


Fig. 5.1 Gamma-ray emission rates and energy release rates for the short irradiation, after 1800 sec cooling time, at position **A**.

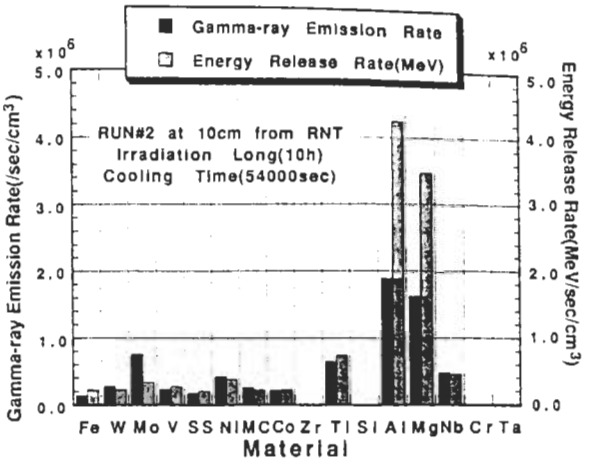


Fig. 5.2 Gamma-ray emission rates and energy release rates for the long irradiation, after 54000 sec cooling time, at position **A**.

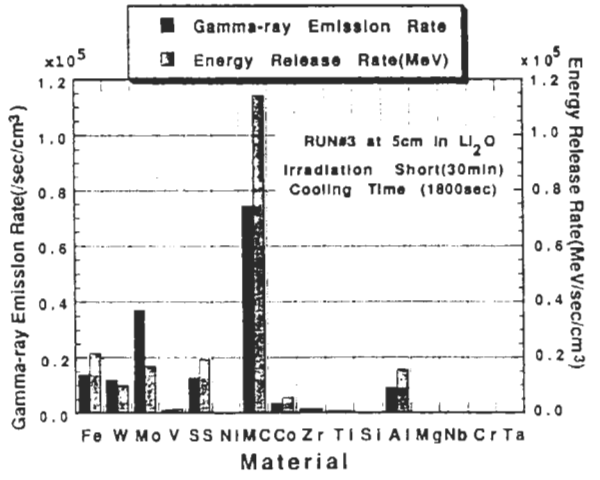


Fig. 5.3 Gamma-ray emission rates and energy release rates for the short irradiation, after 1800 sec cooling time, at position **B**.

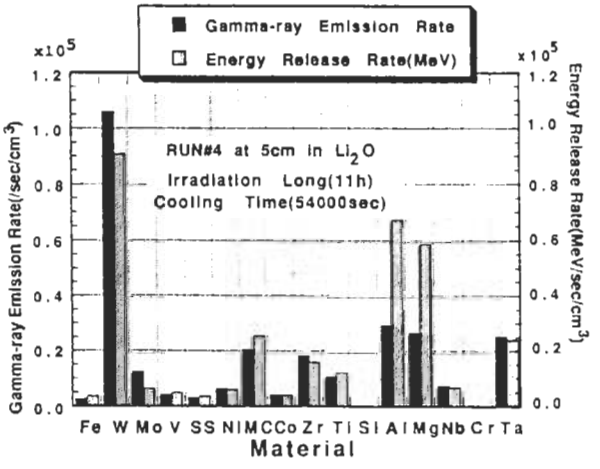


Fig. 5.4 Gamma-ray emission rates and energy release rates for the long irradiation, after 54000 sec cooling time, at position **B**.

section for the 14 MeV neutrons: the production of $^{24}Na(T_{1/2}=15.02h)$ in Al and Mg was not saturated even after 10 h irradiation, beside the production of $^{56}Mn(T_{1/2}=2.579h)$ in Fe, SS-316 and Mn and the production of $^{62}Cu(T_{1/2}=9.73m)$in Cu were already saturated. The same trend are found in the case at position **B** except W. The increase in the γ-ray emission rate for the long irradiation is due to the same reason as in Al case; the half-life of $^{187}W$, dominant activity in W, is 23.9h so that that the production is not saturated after 11h irradiation. The increase rate in the γ-ray is almost in proportion to the total neutron-fluence.

## Decayheat consideration

As shown in Fig 5.1 to 5.4, the values of energy release rates are, in general, in proportion to the intensity of γ-ray emissions. However, Al, Mg, Fe, SS-316 and Co give much larger energy release rates with respect to their γ-ray emission rates in comparison with the other materials. This is simply due to that the $^{24}Na$ and $^{56}Mn$, the dominant activities, emit high energy γ-rays.

Up to now, we devoted discussion on the basis of the γ-ray emission. However, it is worthwhile to consider the β-ray contribution to the energy deposition. Bate energy release rate was deduced from the γ-ray intensity in corporation with the β-decay branching ration per disintegration. Table 4 gives the ratio of the fractions of β-ray in the total energy release rates for respective irradiation runs. It is evident that β-ray have considerable amounts of contribution to the total energy release in a number of materials. They range from a few % to 50 % of the total. They fall, in general, around 20 to 30 % to the

total. The lowest β-contribution was observed in Cr, and next is Ni. The fraction varied with irradiation time as well as cooling times. Especially, the MnCu in the short irradiation at position **A** presented the highest β-ray fraction, because of high Q-β value(3.9 MeV) of $^{62}$Cu. In general, the short lived activity tends to have high Q-β value. This fact indicates the significant importance in the decayheat consideration in the short time range. Thus, productions of short life activities should be taken account into the material selection criteria though the activity disappear in quite short time range. In particular, it is very crucial in operation of fusion device in testing phase because the frequent personnel access for the maintenance is expected and also there should be a large possibility for the accidental failure of the reactor in the early stage of the operation.

Table 4. Contribution of β-ray to the total decay heat

| Materials | β-ray contribution(%) | | | |
|---|---|---|---|---|
| | Run#1 | Run#2 | Run#3 | Run#4 |
| Fe | 28.4 | 28.7 | 29.4 | 26.8 |
| W | 29.1 | 33.3 | 33.1 | 33.6 |
| Mo | 26.8 | 24.7 | 16.0 | 25.0 |
| V | 51.0 | 9.8 | 46.4 | 10.0 |
| SS-316 | 28.9 | 24.1 | 29.3 | 22.1 |
| Ni | 11.6 | 5.0 | 5.1 | 5.2 |
| MnCu | 45.4 | 32.7 | 30.7 | 31.0 |
| Co | 28.9 | 22.0 | 29.9 | 9.8 |
| Zr | 36.9 | ---- | 34.6 | 11.1 |
| Ti | 15.2 | 10.9 | 17.0 | 11.0 |
| Si | 32.4 | ---- | ---- | - - - - |
| Ta | ---- | ---- | ---- | - - - - |

Impurity control

As observed in the spectra of materials of Si and Cr, it happened to yield intensive γ-rays from the unexpected products in the impurities. In some case it is possible to have activities more than 50 % of the total when cross sections of the impurity are orders of magnitude larger than the materials of interest: in soft neutron spectrum, the (n,γ) reaction is significant, while in the 14 MeV dominant field, the (n,2n) reaction takes place with large probability. The results for the Si and Cr are good evidence for this problems we experienced in this study.

## CONCLUSION

The present integral experiment provided data for the verification of the radioactivity calculation code and data. Since all profiles of the radioactivity production and decay are governed by the neutron spectrum and their half-lives, the present analysis provides basic indices for the material selection concerning γ-ray emission characteristics relevant to the dose rate and decayheat estimation in the near term DT fusion device.

## ACKNOWLEDGEMENTS

The US activities are supported by the US Department of Energy, Office of Fusion Energy.

## REFERENCES

1. Y. Ikeda et al.,"An Experimental Study of Induced Activity in Type 316 Stainless Steel by Irradiation in D-T Neutron Fields," JAERI-M 83-177 (1983).
2. Y. Ikeda, et al.,"Measurements of Induced Activity in Type 316 Stainless Steel by Irradiation in D-T Neutron Fields," Fusion Technology., 8, 1466 (1985).
3. K. Oishi, et al.,"Experiment and Analysis of Induced Activities in Concrete Irradiated by 14 MeV Neutrons," Fusion Technology., 10, 579 (1986).
4. K. Oishi, et al.,"Measurement and Analysis of Induced Activities in Concrete Components Irradiated by 14 MeV Neutrons," to be published in Fusion Technology.
5. H. Iida and M. Igarashi,"THIDA Code System for Calculation of the Exposure Dose Rate Around a Fusion Device," JAERI-M 8019 (1978).
6. T. Nakamura, et al.,"A D-T Neutron Source for Fusion Neutronics Experiments as the JAERI," Proc. 7th Int. Conf. Ion Sources and Ion-Assisted Technology and 4th Int. Conf. Ion and Plasma-Assisted Techniques, Kyoto, Japan, Sep. 12-16, 1983.
7. Y. Oyama, et al.,"Measured Characteristics of Be Multi-Layered and Coolant Channel Blankets: Phase-IIC Experiments of the JAERI/USDOE Collaborative on Fusion Neutronis," Presented in this Meeting.
8. A. Kumar, et al.,"Analysis of Induced Activities Measurements Related to Decayheat in Phase-IIC Experimental Assembly: JAERI/USDOE Collaborative Program," Presented in this Meeting.
9. Y. Seki, et al., "THIDA-2: An Advanced Code System for Calculation of Transmutation, Activation, Decay Heat and Dose Rate", JAERI-1301 (1985).
10. F. M. Mann, " REAC2: Status of Codes and Libraries", Technology of Fusion Energy, 8th Topical Meeting, October 1988, Salt Lake City, Fusion Technology, March 1989.
11. D. L. Henderson and O. Yasar,"DKR-ICF: A Radioactivity and Dose Rate Calculation Code Package," Vol. 1 and 2, UWFDM-714 (1986).
12. Y. Seki and H. Iida,"Coupled 42-Group Neutron and 21-Group Gamma-ray Cross Section Sets for Fusion Reactor Calculations," JAERI-M 8818 (1980)
13. H. Baba,"Usage of the BOB 7-Series Program for the Analysis of Ge(Li) Gamma-ray Spectra," JAERI-M 7017 (1977).
14. C. M. Lederer and V. S. Shirley,"Table of Isotopes," Seventh Edition, John Wiley and Sons, Inc., New York (1978).